

## Synchrotron radiation analysis of structure and magnetism of grain boundary phase in Nd-Fe-B sintered magnet

T. Nakamura, A. Yasui, W. Ueno, N. Tsuji, T. Ohkubo\*, H. Iwai\*, T. Akiya\*, Y. Kotani, T. Fukagawa\*\*, T. Nishiuchi\*\*, Y. Gohda\*\*\*, K. Hono\*, and S. Hirosawa\*  
(JASRI/SPring8, \*NIMS, \*\*Hitachi Metals Ltd., \*\*\*Univ. of Tokyo)

A high performance Nd-Fe-B permanent magnet has become an indispensable material for electric products, hybrid vehicles, and power generators, which are key technologies for energy sustainability. Associating with problem on the critical materials, improvement in coercivity without reduction of magnetization is intensely required in Dy-free type Nd-Fe-B magnets. Since it has been known that microstructure is essential for permanent magnets in order to increase the coercivity, the microstructure control may, therefore, bring a solution to developing the high performance Dy-free Nd-Fe-B sintered magnet. In a micro-magnetic point of view, a thin-film-like grain boundary (GB) phase existing between neighboring  $\text{Nd}_2\text{Fe}_{14}\text{B}$  grains is preferred to be paramagnetic so as to prevent reversed magnetic domains from expanding into neighboring grains. Although the GB phase had been believed to be paramagnetic for a long time, the recent study using a three dimensional laser atom probe technique by Sepehri-Amin *et al.* showed convincing results indicating that the amorphous GB phase could be ferromagnetic [1]. Further studies on magnetism of the GB phase, however, are needed to uncover the origin of the coercivity.

In the present work, we have measured X-ray magnetic circular dichroism (XMCD) spectra in a  $\text{Nd}_{14.0}\text{Fe}_{79.7}\text{B}_{6.2}\text{Cu}_{0.1}$  sintered magnet using synchrotron soft X-rays at BL25SU of SPring-8 in order to clarify the magnetic state of the GB phase. Since the Nd-Fe-B sintered magnets have a grain-boundary fracturing character, magnetism of the GB is directly investigated by the surface-sensitive XMCD measurement using a total electron yield (TEY) method [2]. The XMCD of the Fe  $L_{2,3}$ -edges was measured on the fractured surface which was covered with the GB phase. Applying the magneto optical sum rule [3-5], the apparent Fe magnetic moment was obtained as  $1.66 \mu_B$  from the XMCD spectra measured at  $30^\circ\text{C}$ . Since the recorded XMCD signal was composed of those coming from the GB phase and the under-layered  $\text{Nd}_2\text{Fe}_{14}\text{B}$  main phase, the magnetic moment of  $1.66 \mu_B$  was deconvoluted into each contribution on assumption of the probing depth of the TEY ( $\lambda_e=1.2 \text{ nm}$ ) at the Fe  $L_{2,3}$ -edges [2] and a thickness of the GB phase ( $t_B=3 \text{ nm}$ ) [1]. As the result of the deconvolution analysis, the Fe magnetic moment of the GB phase was estimated as  $1.4 \mu_B$ . This value is of about 60 % compared to that of  $\text{Nd}_2\text{Fe}_{14}\text{B}$  and implies that the GB phase is ferromagnetic. Moreover, the temperature dependence of Fe magnetic moment in Fig. 1, which was obtained from the XMCD spectra, indicated that the Curie temperature of the GB phase was lower than that of the main phase,  $\text{Nd}_2\text{Fe}_{14}\text{B}$ . The present result, therefore, implies that the coercivity will possibly be improved by forming the GB phase which has the Curie point being lower than the operating temperature.

It was reported that the thin-film-like GB phase grows by post-sintered annealing process [1]. The materials to form the GB phase could be supplied from somewhere like the Nd-rich phase at the triple junction during the annealing process. In order to elucidate the metallurgical phenomena with respect to the constitutional phases, we have investigated the crystal phases in the  $\text{Nd}_{14.0}\text{Fe}_{79.7}\text{B}_{6.2}\text{Cu}_{0.1}$  sintered magnet by X-ray diffraction (XRD) experiment up to  $1000^\circ\text{C}$ . High temperature *in-situ* XRD measurements were performed at BL02B2 of SPring-8. In

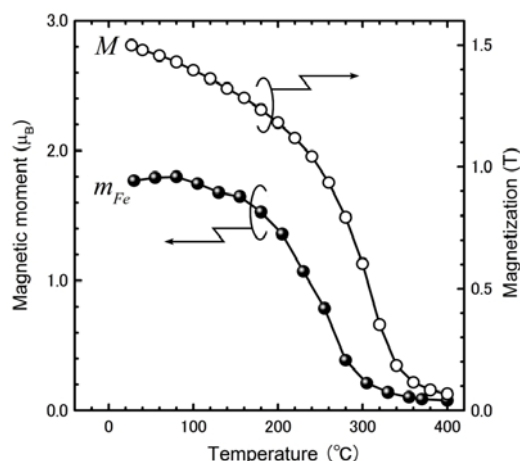


Fig. 1 Temperature dependence of Fe magnetic moments ( $m_{Fe}$ ) obtained by sum rule analysis of XMCD spectra at the Fe  $L_{2,3}$ -edges and a magnetization ( $M$ ). Both XMCD and magnetization were measured under 1.9 T.

previous studies by means of transmission electron microscopy (TEM) [6, 7], it has been reported that the Nd-rich phase is a mixture of Nd ( $P6_3/mmc$ ),  $Nd_2O_3$  ( $P6_3/mmc$ ),  $NdO_x$  ( $Fm\bar{3}m$ ), and small amounts of other compounds, where symbols in parentheses denote the space groups of crystallography. Among them, the Nd-metal phase is expected to relate to the formation of the GB phase because the optimum annealing temperature of 540 °C is very close to the eutectic point of 520 °C in the Cu-Nd system. Fig. 2 shows temperature dependence of XRD patterns with labels denoting crystal phases determined by analysis of the XRD patterns. The Nd-metal phase ( $P6_3/mmc$ ) starts melting at 580 °C (XRD pattern at 580 °C is not shown here), and completely melts at 606 °C. The melting point of the metallic Nd phase in the present experiment is higher than that expected from the eutectic point by 60 ~ 80 °C. This difference of the temperature is explained as that the XRD detects the crystalline Nd-metal unused in the eutectic reaction because the Cu concentration (0.1 at%) is too small to consume all of the crystalline Nd phases (>1 at%). Here, the volume fraction of Nd which exists as Nd metal was estimated from the Rietvelt analysis of XRD pattern. On the other hand, a different Nd phase having cubic crystal symmetry ( $Fm\bar{3}m$ ) was also found in the temperature range between 335 ~ 788 °C. Variation in volume fraction of the cubic and hexagonal phases of Nd was invisible at the eutectic point. The  $Nd_2O_3$  phase remains solid state even at 1000 °C, but shows some phase transitions with respect to crystal symmetries involving  $P6_3/mmc$ ,  $Ia\bar{3}$ , and  $P\bar{3}m1$ . Although the mechanism of these phase transitions in the  $Nd_2O_3$  phases is still not clear, the information may be useful in refining the Nd-O phase diagram which is important in elucidation of the microstructural formation mechanism of Nd-Fe-B magnets.

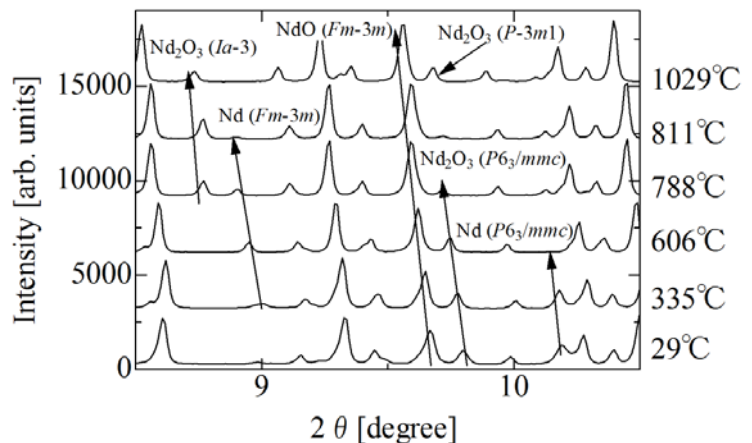


Fig. 2 Temperature dependence of XRD patterns of  $Nd_{14.0}Fe_{79.7}B_{6.2}Cu_{0.1}$  sintered magnet. Arrows beside XRD peaks denote trends of shift of peak positions for identified crystalline phases.

### Acknowledgements

The authors are grateful to Drs. J. Kim, K. Sugimoto, M. Suzuki, A. Fujiwara, and M. Takata of JASRI, and Dr. H. Sepehri-Amin and T. Abe of NIMS for fruitful discussions. A part of this work is supported by the Elements Strategy Initiative Center for Magnetic Materials under the outsourcing project of MEXT.

### References

- [1] H. Sepehri-Amin, T. Ohkubo, T. Shima, K. Hono, *Acta Mater.* **60**, 819 (2012).
- [2] B. H. Frazer, B. Gilbert, B. R. Sonderegger, and G. De Stasio, *Surf. Sci.* **537**, 161 (2003).
- [3] B. T. Thole, P. Carra, F. Sette, and G. van der Laan, *Phys. Rev. Lett.* **68**, 1943 (1992).
- [4] P. Carra, B. T. Thole, M. Altarelli, and X. Wang, *Phys. Rev. Lett.* **70**, 694 (1993).
- [5] C. T. Chen, Y. U. Idzerda, H. -J. Lin, N. V. Smith, G. Meigs, E. Chaban, G. H. Ho, E. Pellegrin, and F. Sette, *Phys. Rev. Lett.* **75**, 152 (1995).
- [6] J. Fidler, *IEEE Trans. Magn.* **21**, 1955 (1985).
- [7] Mo W, Zhang L, Liu Q, Shan A, Wu J, Komuro M. *Scripta Mater.* **59**, 179 (2008).